

# Redox features in the catalytic mechanism of the “standard” and “fast” NH<sub>3</sub>-SCR of NO<sub>x</sub> over a V-based catalyst investigated by dynamic methods

Enrico Tronconi <sup>a,\*</sup>, Isabella Nova <sup>a</sup>, Cristian Ciardelli <sup>a</sup>, Daniel Chatterjee <sup>b</sup>, Michel Weibel <sup>b</sup>

<sup>a</sup> Dipartimento di Chimica, Materiali e Ingegneria Chimica “G. Natta”, Politecnico di Milano, Piazza Leonardo da Vinci 32, I-20133 Milano, Italy

<sup>b</sup> DaimlerChrysler AG Abteilung RBP/C, HPC: 096-E220, D-70546 Stuttgart, Germany

Received 29 June 2006; revised 20 August 2006; accepted 12 September 2006

Available online 16 October 2006

## Abstract

The redox mechanism governing the selective catalytic reduction (SCR) of NO/NO<sub>2</sub> by ammonia at low temperature was investigated by transient reactive experiments over a commercial V<sub>2</sub>O<sub>5</sub>/WO<sub>3</sub>/TiO<sub>2</sub> catalyst for diesel exhaust aftertreatment. NO + NH<sub>3</sub> temperature-programmed reaction runs over reduced catalyst samples pretreated with various oxidizing species showed that both NO<sub>2</sub> and HNO<sub>3</sub> were able to reoxidize the V catalyst at much lower temperature than gaseous O<sub>2</sub>: furthermore, they significantly enhanced the NO + NH<sub>3</sub> reactivity below 250 °C via the buildup of adsorbed nitrates, which act as a surface pool of oxidizing agents but are decomposed above that temperature. Both such features, which were not observed in comparative experiments over a V-free WO<sub>3</sub>/TiO<sub>2</sub> catalyst, point out a key catalytic role of the vanadium redox properties and can explain the greater deNO<sub>x</sub> efficiency of the “fast” SCR (NO + NH<sub>3</sub> + NO<sub>2</sub>) compared with the “standard” SCR (NO + NH<sub>3</sub> + O<sub>2</sub>) reaction. A unifying redox approach is proposed to interpret the overall NO/NO<sub>2</sub>-NH<sub>3</sub> SCR chemistry over V-based catalysts, in which vanadium sites are reduced by the reaction between NO and NH<sub>3</sub> and are reoxidized either by oxygen (standard SCR) or by nitrates (fast SCR), with the latter formed via NO<sub>2</sub> disproportionation over other nonreducible oxide catalyst components.

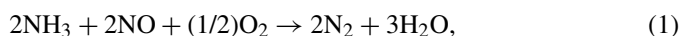
© 2006 Elsevier Inc. All rights reserved.

**Keywords:** Diesel-urea SCR; Selective catalytic reduction; Standard SCR; Fast SCR; Redox properties; Redox catalytic kinetics; Dynamic methods

## 1. Introduction

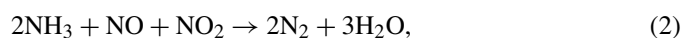
Selective catalytic reduction (SCR) with NH<sub>3</sub>/urea is emerging as the most promising technology for the abatement of NO<sub>x</sub> emissions from diesel vehicles [1–8]. This has stimulated a renewed interest in investigating the fundamental aspects of SCR catalytic chemistry, also in view of the need for the transportation industry to develop design and simulation tools incorporating suitable SCR kinetic schemes.

Indeed, NH<sub>3</sub> SCR over vanadia-type catalysts, in which 1 molecule of NO is reduced by 1 molecule of ammonia in the presence of oxygen to give dinitrogen and water,



has represented for the last two decades the most effective commercial deNO<sub>x</sub>ing process for stack gases from power plants

and other stationary sources [9]. However, the specific demands of mobile applications, associated with, for example, volume limitations and dynamic operation, do not permit straightforward transposition of the technology. Because the working conditions for mobile applications may be much colder than in stationary installations, increasing the deNO<sub>x</sub> activity at low temperatures represents a major development goal. A possible solution to this issue is represented by the so-called “fast” SCR reaction known since the early 1980s, when Kato et al. [10] found that the reaction involving an equimolar NO and NO<sub>2</sub> feed mixture,



is significantly faster than the “standard” SCR, reaction (1), at low temperature. In practical terms, a preoxidation catalyst located upstream of the SCR catalyst could convert a fraction of NO in the engine exhausts to NO<sub>2</sub> to approach the optimal NO/NO<sub>2</sub> equimolar feed ratio of reaction (2) [11]. Nevertheless, adding NO<sub>2</sub> to the SCR reacting system introduces consid-

\* Corresponding author. Fax: +39 02 2399 3318.

E-mail address: [enrico.tronconi@polimi.it](mailto:enrico.tronconi@polimi.it) (E. Tronconi).

erable complexity resulting from the multiplication of primary and secondary reaction routes and may result in the formation of such undesired byproducts as  $\text{NH}_4\text{NO}_3$  and  $\text{N}_2\text{O}$  [12,13]. From a more fundamental standpoint, the relationship between the catalytic chemistry of the standard SCR and that of the less well-investigated fast SCR, as well as the reasons why  $\text{NO}_2$  dramatically accelerates the reduction of  $\text{NO}$  by ammonia, have not yet been fully elucidated.

Because of its widespread application in the abatement of  $\text{NO}_x$  emissions from stationary sources, the mechanism of the standard SCR reaction has been extensively investigated [9,14]. It is generally agreed that the reaction proceeds according to a redox scheme, in which gaseous oxygen is needed for reoxidation of the V-related catalyst sites reduced by the reaction between  $\text{NO}$  and  $\text{NH}_3$ . It is also established that at low temperature, the catalyst reoxidation by gas-phase oxygen is the rate-determining step of the overall reaction mechanism [15–20].

Concerning the fast SCR reaction (2), a much more limited number of papers analyzing the  $\text{NH}_3$ – $\text{NO}/\text{NO}_2$  reacting system are available in the scientific literature. This field was pioneered by Koebel and co-workers [11,17,21,22], who extensively investigated the reactivity of  $\text{NH}_3$ – $\text{NO}/\text{NO}_2$  over powdered and monolithic vanadia-based catalysts. Addressing possible reasons for the observed higher rates of the fast SCR reaction at low  $T$ , they proposed that gaseous  $\text{NO}_2$  would replace oxygen as a more effective oxidizing agent, thus allowing faster reoxidation of the vanadium sites. The  $\text{NO}_2$ -enhanced reoxidation of the catalyst was demonstrated by in situ Raman experiments over  $\text{V}_2\text{O}_5/\text{TiO}_2$  [17], but no direct kinetic evidence was provided to confirm that this effect could explain the order-of-magnitude increment of the SCR. Moreover, a mechanistic scheme in which  $\text{NO}_2$  simply replaces oxygen in reoxidizing the V sites cannot account for the significant role played by other species in the  $\text{NO}/\text{NO}_2$ – $\text{NH}_3$  system. Recently we showed by transient experiments over a commercial V-based catalyst that the reduction of nitrate species (related to previously deposited ammonium nitrate formed by reaction between  $\text{NO}_2$  and  $\text{NH}_3$ ) by nitric oxide proceeds at the same rate as the fast SCR at  $170^\circ\text{C}$  [23,24]. This suggests that such a reaction pathway may be involved (and actually be rate-controlling) in the low-temperature catalytic mechanism of the fast SCR reaction over V-based catalysts. Such data have been rationalized according to a reaction scheme in which  $\text{NO}_2$  forms nitrite and nitrate species by disproportion,  $\text{NO}$  reduces nitrates to nitrites, and  $\text{NH}_3$  reacts with nitrites to form unstable ammonium nitrite, which readily decomposes to nitrogen and water [24]. Similar indications, obtained in this case mostly by spectroscopic techniques, have been reported by Sachtler and co-workers for  $\text{NO}/\text{NO}_2$ – $\text{NH}_3$  SCR over zeolite catalysts [25]. This scheme is able to account for an extensive set of kinetic observations, including the influence of the  $\text{NO}/\text{NO}_2$  feed ratio on the selectivities to  $\text{N}_2$ ,  $\text{NH}_4\text{NO}_3$ , and  $\text{N}_2\text{O}$  [13]; however, it does not explicitly reflect the redox nature of the catalytic mechanism of SCR.

Herein we address redox mechanistic features of standard SCR and fast SCR over an industrial  $\text{V}_2\text{O}_5$ – $\text{WO}_3/\text{TiO}_2$  catalyst for mobile applications, considered a representative V-

based SCR catalyst with optimized composition. The reactivity of  $\text{NO} + \text{NH}_3$  in the low-temperature range is investigated by temperature-programmed reduction (TPR) methods under conditions typical of real aftertreatment devices over catalyst samples subjected to various pretreatments, to examine the influence of different reducing and oxidizing agents on SCR activity. Specifically, the relation between surface nitrates and the redox mechanism of fast SCR is explored. Comparative experiments over a V-free  $\text{WO}_3/\text{TiO}_2$  catalyst are also performed to identify the catalytic role of vanadium.

## 2. Materials and methods

Unsteady SCR reactive experiments were performed at  $50$ – $250^\circ\text{C}$  over a commercial extruded  $\text{V}_2\text{O}_5$ – $\text{WO}_3/\text{TiO}_2$  catalyst ( $A_s \approx 70 \text{ m}^2/\text{g}$ ) with intermediate V content, originally supplied as a honeycomb monolith. A significant portion of the catalyst was crushed and ground to powder (140–200 mesh); for each experiment, a small sample (160 mg) was collected from the mixed powders, diluted with 80 mg of quartz, and loaded in a flow microreactor consisting of a quartz tube (6 mm i.d.). Using the same procedures, a commercial  $\text{WO}_3/\text{TiO}_2$  catalyst (Thann et Mulhouse S.A.) was also tested in specific runs for comparison purposes.

The test reactor was operated at atmospheric pressure with a total flow rate of either 120 or 280  $\text{cm}^3/\text{min}$  (STP), corresponding to a gas hourly space velocity (GHSV) of about  $9 \times 10^4$  or  $2.1 \times 10^5 \text{ h}^{-1}$ , respectively. Diluted gas streams of  $\text{NO}$ ,  $\text{NO}_2$ ,  $\text{NH}_3$ , and  $\text{O}_2$  in He from bottled calibrated mixtures were mixed in suitable proportions by means of mass flow controllers (Brooks 5850 E) to achieve the desired feed composition for each run. For  $\text{H}_2\text{O}$ -containing feeds, the feed stream was passed through a saturator maintained at a controlled temperature before entering the microreactor. For catalyst pretreatment with  $\text{HNO}_3$ , the feed stream was saturated with a suitable aqueous solution of nitric acid.

The reactor outlet was directly connected to both a UV analyzer (ABB Limas 11-HW) and a quadrupole mass spectrometer (Balzers QMS 200) operating in parallel. In each experiment, the UV analyzer monitored the temporal evolution of the outlet  $\text{NO}$ ,  $\text{NO}_2$ , and  $\text{NH}_3$  concentrations. Helium was used as the carrier gas, so that nitrogen (the main SCR product) could be detected by the MS, along with the byproduct  $\text{N}_2\text{O}$ , thus allowing evaluation of overall N balances, which always closed within  $\pm 5\%$  at steady state. As a consistency check, the outlet concentration traces of  $\text{NO}$ ,  $\text{NO}_2$ , and  $\text{NH}_3$  also were estimated from the MS signals after proper calibration; the steady-state levels agreed satisfactorily with those measured by the UV analyzer, whereas the transient phases were typically associated with a slower MS response, particularly in the case of ammonia. In view of the purposes of the present work, herein we primarily report the outlet concentration traces of  $\text{NO}$  generated by the UV analyzer.

Typical experiments were  $\text{NO} + \text{NH}_3$  TPR runs. A feed stream consisting of  $\text{NH}_3$  (1000 ppm) +  $\text{NO}$  (1000 ppm) with  $\text{H}_2\text{O}$  (1% v/v), balance He, and no oxygen was initially admitted to the reactor at  $50^\circ\text{C}$ . Then the catalyst temperature

was continuously increased at 20 °C/min up to 250–550 °C, depending on the purposes of the experiment. Such TPR experiments were carried out over reference reduced and oxidized catalyst samples, as well as over other catalyst samples subjected to different pretreatments.

The reference reduced catalyst samples were obtained by exposure to NH<sub>3</sub> (1000 ppm feed stream) at 550 °C for about 1.5 h. Catalyst reduction was confirmed by a peak of N<sub>2</sub> evolution during the first few minutes, the integral amount of which was compatible with reduction of the vanadium catalyst load. The reference oxidized catalyst samples were obtained by exposure to O<sub>2</sub> (500 ppm) during a temperature ramp (20 °C/min) up to 550 °C; oxidation of the catalyst was confirmed by O<sub>2</sub> consumption and H<sub>2</sub>O evolution at temperatures above ca. 200 °C.

Various other pretreatments were also applied to the catalyst to investigate their influence on its oxidation state and its SCR reactivity, as discussed in the following sections. Specifically, pretreatment procedures were performed by feeding H<sub>2</sub>O (1% v/v) in a temperature ramp up to 550 °C, H<sub>2</sub>O (1% v/v) at 200 °C, NO (1000 ppm) at 200 °C, NO (1000 ppm) + H<sub>2</sub>O (1% v/v) at 200 °C, NH<sub>3</sub> (1000 ppm) at 200 °C, NO (1000 ppm) + NH<sub>3</sub> (1000 ppm) at 200 °C, NO<sub>2</sub> (100 or 500 ppm) at 150 °C, and HNO<sub>3</sub> (about 100 ppm) + H<sub>2</sub>O (1% v/v) at 100, 150, and 200 °C.

In addition to TPR runs, specific tests were carried out according to the transient response method (TRM experiments). This involved performing a step change of the inlet concentration of one reactant (1000 ppm NH<sub>3</sub>, NO, or NO<sub>2</sub>) while feeding other reactants in the presence of H<sub>2</sub>O (1% v/v) and balance He at 170 °C. In line with the SCR literature for V-based systems [14], no significant activity in the oxidation of NO to NO<sub>2</sub> up to 450 °C was observed over the present catalysts, even in dedicated diagnostic runs.

### 3. Results and discussion

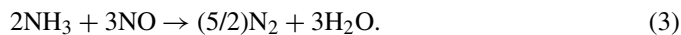
#### 3.1. SCR behavior of reference reduced and reference oxidized catalyst samples

The activity in the standard SCR reaction of reference reduced and oxidized catalyst samples was first analyzed by NO + NH<sub>3</sub> TPR. Over the reference reduced catalyst, no conversion of NO was evident up to 200 °C, and only minor SCR activity was apparent at 250 °C, when about 980 ppm of NO was still present in the outlet stream.

A different picture was observed for NO + NH<sub>3</sub> TPR over the reference oxidized catalyst. The NO outlet concentration began to decrease at ≈130 °C, and the NO conversion was close to 8% at 250 °C. Occurrence of the SCR reaction was also confirmed by stoichiometric evolution of nitrogen, the integral amount of which was found to be in good agreement with that measured during reference reduction of the catalyst sample.

The data were reproducible, as confirmed by several replicated runs over both prerduced and preoxidized catalyst samples. The data indicate that the reduced commercial V catalyst is virtually inactive in the standard SCR reaction when no oxy-

gen is present in the feed stream; the minor NO conversions measured above 200 °C are attributed to the so-called “slow” SCR reaction [12,14],



In fact, replicated temperature ramps performed up to higher temperatures over the reduced catalyst confirmed conversion of both nitric oxide and ammonia, as well as production of nitrogen, according to the stoichiometry of reaction (3). It is well known that under practical conditions, that is when oxygen is present, slow SCR is negligibly slow compared with standard SCR.

In contrast, the catalyst sample pretreated according to the reference oxidizing procedure appeared to be significantly more active. Indeed, analysis of the outlet concentrations of nitric oxide, ammonia, and nitrogen confirmed the occurrence of the standard SCR reaction (1) at temperatures as low as 130 °C. This is in line with literature reports [15] that standard SCR over V-based catalysts proceeds by consuming the catalyst lattice oxygen, in agreement with a redox mechanism. If oxygen is fed to the reactor, then the lattice oxygen consumed by the reaction can be replenished, and the reaction proceeds to steady state. Otherwise (i.e., if gaseous oxygen is not available), the reaction stops once all of the reactive lattice oxygen of the catalyst is depleted [15]. In fact, starting from around 250 °C, the evolution of NO conversion measured over the reference oxidized catalyst increased only slowly, paralleling that observed over the reference reduced catalyst, thus indicating that only the slow SCR reaction (3) was proceeding.

#### 3.2. Standard SCR reaction versus catalyst reoxidation

We now apply the tests assessed in the previous section to clarify aspects of the redox mechanism associated with the standard SCR reaction. Fig. 1 illustrates results from three different TPR runs: (A) NO concentration profile during NO + NH<sub>3</sub> + O<sub>2</sub> TPR over a reference reduced catalyst, (B) O<sub>2</sub> concentration profile during a temperature ramp for reoxidation of a reference reduced catalyst, and (C) NO concentration profile during NO + NH<sub>3</sub> + O<sub>2</sub> TPR over a WO<sub>3</sub>/TiO<sub>2</sub> catalyst.

It is apparent that curve (B), although very noisy due to experimental limitations with the signal acquisition from the MS, essentially overlaps curve (A). Accordingly, the same activation threshold prevailed for both reoxidation of a reference reduced catalyst (curve (B)) and standard SCR in the presence of gaseous oxygen over a reference reduced catalyst (curve (A)). In contrast, the NO + NH<sub>3</sub> + O<sub>2</sub> TPR experiment over the V-free catalyst (curve (C)) showed the onset of some NO conversion only above roughly 300 °C, a threshold temperature well above that measured for the V-based catalyst, thus confirming that the low-temperature activity in the standard SCR reaction can be ascribed to the well-known redox properties of the vanadium catalyst component [9,12,14].

Accordingly, the data in Fig. 1 support that V reoxidation is the rate-limiting step in the standard SCR reaction. Of course, such a result has significant implications for SCR kinetic modeling and is in agreement with indications reported previously.

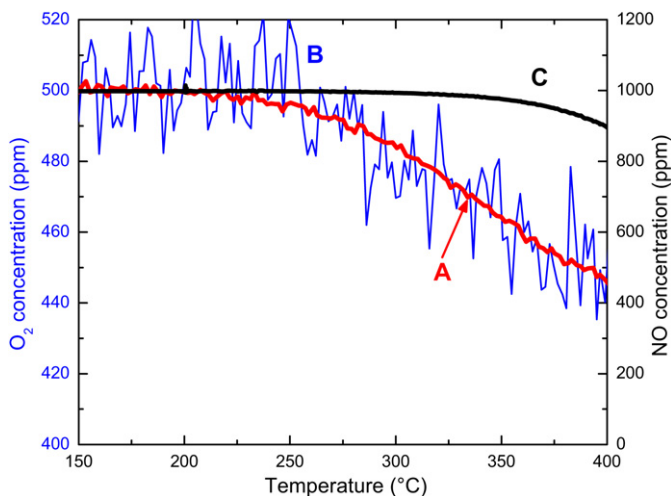


Fig. 1. Curve (A) NO concentration profile during NO + NH<sub>3</sub> + O<sub>2</sub> (1000/1000/500 ppm + He) TPR over a reference reduced catalyst. Curve (B) O<sub>2</sub> concentration profile during reoxidation (O<sub>2</sub> feed = 500 ppm + He) of a reference reduced catalyst. Curve (C) NO concentration profile during NO + NH<sub>3</sub> + O<sub>2</sub> (1000/1000/20,000 ppm + He) TPR over a WO<sub>3</sub>/TiO<sub>2</sub> catalyst; flow rate = 280 cm<sup>3</sup>/min (STP). Heating rate = 20 °C/min.

Using different approaches, Lietti and Forzatti [15] and Marshneva et al. [20] concluded that the slow step in the SCR reaction over V<sub>2</sub>O<sub>5</sub>-WO<sub>3</sub>/TiO<sub>2</sub> catalysts is associated with V catalyst oxidation by gaseous oxygen.

Having established the redox nature of the standard SCR reaction, we next assess the roles of different species in the related reduction and oxidation steps, respectively.

### 3.3. Activities of different species in catalyst reduction

To identify the species responsible for catalyst reduction during the standard and fast SCR reactions, we studied the activity of different potential reducing agents participating in the SCR reacting system (NO, NH<sub>3</sub>, H<sub>2</sub>O, and combinations thereof), according to the following procedure. A fresh catalyst sample was first oxidized, then pretreated with one of the candidate reducing agents. After the pretreatment, NO + NH<sub>3</sub> TPR was run, and the resulting NO reduction activity was compared with the corresponding data obtained over both the reference oxidized and reduced catalysts.

The results are summarized in Fig. 2, which compares the NO reduction activity in the TPR runs performed over the catalyst samples after various pretreatments. Specifically, such pretreatments involved feeding H<sub>2</sub>O (1% v/v) at 200 °C (curve (A)), H<sub>2</sub>O (1% v/v) at a temperature ramp up to 550 °C (curve (B)), NO (1000 ppm) at 200 °C (curve (C)), NH<sub>3</sub> (1000 ppm) at 200 °C (curve (D)), NO (1000 ppm) + H<sub>2</sub>O (1% v/v) at 200 °C (curve (E)), and NO + NH<sub>3</sub> (1000 + 1000 ppm) at 200 °C (curve (F)). In addition, curves obtained for the reference oxidized (curve (G)) and of the reference reduced (curve (H)) catalyst samples are reported for comparison.

Fig. 2 shows that in curves (A)–(E), the observed deNO<sub>x</sub> activity was essentially identical to that typical of the reference oxidized catalyst (curve (G)) and remained evidently higher than the activity measured over the reference reduced cata-

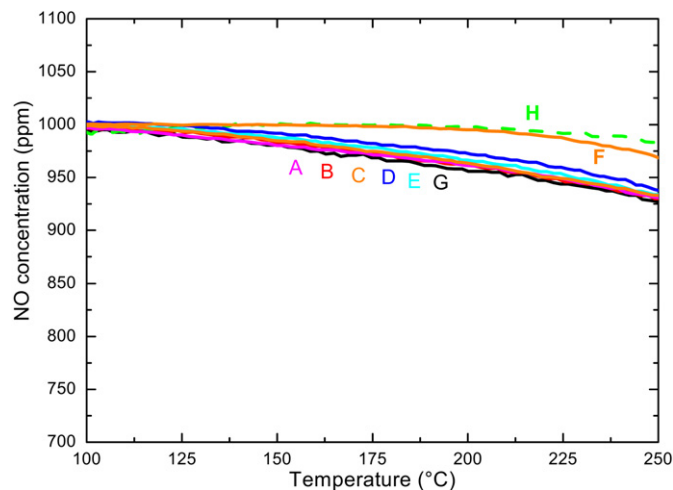


Fig. 2. NO concentration profiles during NO + NH<sub>3</sub> TPR (1000/1000 ppm + He) over catalysts after different pretreatments: (A) H<sub>2</sub>O (1% v/v) at 200 °C; (B) H<sub>2</sub>O (1% v/v) in *T*-ramp up to 550 °C; (C) NO (1000 ppm) at 200 °C; (D) NH<sub>3</sub> (1000 ppm) at 200 °C; (E) NO (1000 ppm) + H<sub>2</sub>O (1% v/v) at 200 °C; (F) NO (1000 ppm) + NH<sub>3</sub> (1000 ppm) at 200 °C; (G) reference oxidized catalyst; (H) reference reduced catalyst. Other conditions as in Fig. 1.

lyst (curve (H)). Thus, it appears that exposure of the oxidized catalyst to atmospheres containing either H<sub>2</sub>O or NO or NH<sub>3</sub> alone or H<sub>2</sub>O + NO together at 200 °C did not reduce the catalyst. H<sub>2</sub>O did not reduce the oxidized catalyst even at 550 °C. Further supporting this conclusion is the fact that no nitrogen evolution was detected during all such pretreatments.

In contrast, curve (F) in Fig. 2 shows the results of a similar experiment over an oxidized catalyst sample that had been exposed to a mixture of NO and NH<sub>3</sub> (1000 + 1000 ppm) at 200 °C before the TPR run. In this case, deNO<sub>x</sub> activity was quite similar to that observed over the reference reduced catalyst (curve (H)); moreover, N<sub>2</sub> evolution was observed during the pretreatment. Although additional spectroscopic evidence would be needed in this respect, these data suggest that NO + NH<sub>3</sub> jointly were able to reduce the present V catalyst already at 200 °C. This indeed seems consistent with the results in Fig. 1. As discussed in the previous section, at 200 °C, SCR activity is limited by catalyst reoxidation, whereas the reduction step of its redox mechanism was found to proceed already rapidly at the same temperature.

### 3.4. Mechanistic implications: catalyst reduction

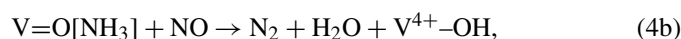
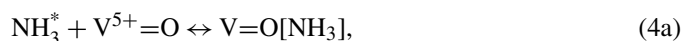
In this section we briefly discuss some mechanistic implications of the present results concerning the catalyst reduction phase in the redox mechanism of the standard and fast SCR reactions. Our data do not support a direct reducing action of NO alone. This is in agreement with the view, supported by many authors, that NH<sub>3</sub> rather than NO is activated (i.e., oxidized) by V-based catalysts in the first step of the standard SCR catalytic mechanism [14]. Our data also do not support that at 200 °C, ammonia alone is directly activated by deeply reducing the V catalyst. In fact, as suggested by Fig. 2 and by the data on N<sub>2</sub> evolution during catalyst pretreatment, under the present experimental conditions, the catalyst reduction step in the redox SCR



mechanism seems to require a cooperative action (co-presence) of both NO and NH<sub>3</sub>. In this respect it should be also considered that the reducing action of NH<sub>3</sub> is enabled by the presence of V atoms in adjacent sites [26,27]; however, exploring the affect of V surface density is beyond the scope of the present study.

The foregoing results may be consistent with the following interpretations:

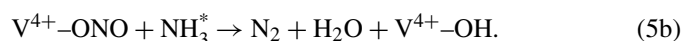
1. Ammonia, already adsorbed onto nonreducible acidic sites, is initially activated (oxidized) by adjacent vanadium redox sites, but the reaction proceeds to a significant extent only after interaction with gaseous NO according to an Eley–Rideal scheme,



where NH<sub>3</sub><sup>\*</sup> represents adsorbed ammonia.

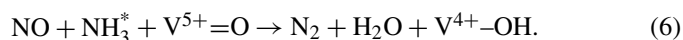
A similar proposal was formulated by Topsøe et al. on the basis of in situ FTIR evidence [19]. However, the chemical nature of the initial NH<sub>3</sub> activation, which does not reduce the catalyst deeply (with nitrogen evolution), as documented herein, remains to be clarified. Moreover, this interpretation is somewhat at variance with recent kinetic data showing considerable inhibition of ammonia on the low-temperature SCR of NO and pointing to the existence of an optimal NH<sub>3</sub> surface coverage [18,28–31]. It was also found that such an inhibiting action of ammonia, already reported by other authors [32–34], cannot be accommodated by a simple Eley–Rideal kinetic approach assuming a reaction between adsorbed ammonia and gaseous nitric oxide [18,30].

2. Nitric oxide is oxidized by the V catalyst to nitrite species, but the equilibrium is highly unfavorable and shifts to the right only in the presence of NH<sub>3</sub> (adsorbed onto nearby acidic sites), which reacts with nitrites to give N<sub>2</sub> and H<sub>2</sub>O via decomposition of unstable ammonium nitrite intermediates, for example, according to

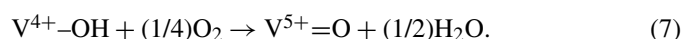


In this case, the inhibiting action of ammonia could be more easily explained by either a competitive adsorption of NH<sub>3</sub> onto the V sites involved in NO activation or an adverse electronic interaction of adsorbed NH<sub>3</sub> with the vanadium oxidizing centers [18].

In any case, both (4a) + (4b) and (5a) + (5b) yield the overall catalyst reduction step,



For the standard SCR reaction, reoxidation of the reduced V sites closing the redox cycle is then carried out by gaseous oxygen according to



For fast SCR, however, other strong oxidizing agents—namely, NO<sub>2</sub> and HNO<sub>3</sub>—are present in the reacting environment in addition to O<sub>2</sub>. Thus, it is of interest to compare their oxidizing activity, as we discuss in the following sections.

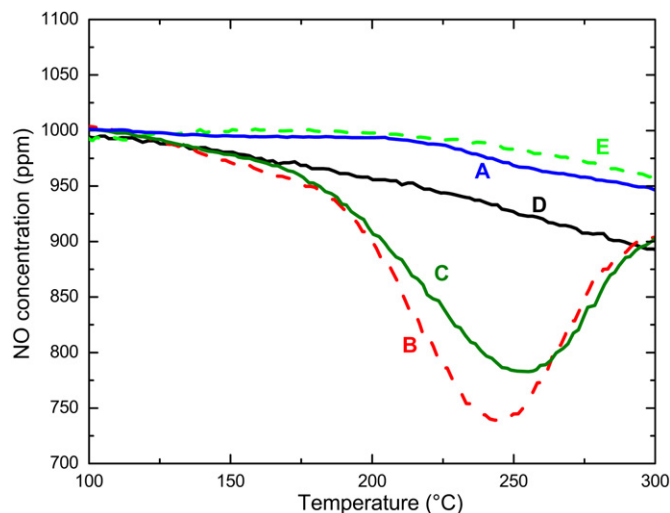


Fig. 3. NO concentration profiles during NO + NH<sub>3</sub> TPR over catalysts after different pretreatments: (A) O<sub>2</sub> (500 ppm) at  $T = 150^\circ\text{C}$ ; (B) NO<sub>2</sub> (100 ppm) at  $150^\circ\text{C}$ ; (C) HNO<sub>3</sub> (~100 ppm) at  $150^\circ\text{C}$ ; (D) reference oxidized catalyst; (E) reference reduced catalyst. Other conditions as in Fig. 1.

### 3.5. Activity of different species in catalyst reoxidation

Similar to the investigation of reducing agents in Section 3, in this section we test the reactivity of different oxidizing species, namely O<sub>2</sub>, NO<sub>2</sub>, and HNO<sub>3</sub>, in the catalyst reoxidation step of the redox SCR mechanism. Fig. 3 compares the deNO<sub>x</sub> activity observed in NO + NH<sub>3</sub> TPR runs over three catalyst samples. Each sample was first reduced according to the reference procedure, then pretreated at  $150^\circ\text{C}$  with a different oxidizing agent—O<sub>2</sub> (curve (A)), NO<sub>2</sub> (curve (B)), or HNO<sub>3</sub> (curve (C))—and finally tested in a NO + NH<sub>3</sub> TPR run. Data collected in the same TPR experiment over the reference oxidized catalyst sample (curve (D)) and the reference reduced catalyst sample (curve (E)) also are displayed for comparison.

It is apparent from Fig. 3 that the NO evolution recorded when the catalyst sample was pretreated in oxygen flow at  $150^\circ\text{C}$  (curve (A)) essentially overlaps with the curve obtained over the reference reduced catalyst (curve (E)): hence, oxygen was apparently unable to reoxidize the prerduced V catalyst at  $150^\circ\text{C}$ . This is consistent with the data in curve (B) of Fig. 1, which suggest that the onset of catalyst reoxidation by oxygen occurred above  $200^\circ\text{C}$  under our experimental conditions.

In contrast, NO evolution traces recorded after exposing the reduced catalyst both to NO<sub>2</sub> (curve (B)) and to HNO<sub>3</sub> (curve (C)) show that NO conversion was initiated already at about  $130^\circ\text{C}$ , a threshold temperature very similar to that typical of the reference oxidized catalyst (curve (D)). These data then suggest that both NO<sub>2</sub> and HNO<sub>3</sub> were able to effectively reoxidize the V catalyst at  $150^\circ\text{C}$ .

Notably, two similar TPR experiments were repeated after exposing prerduced catalyst samples to HNO<sub>3</sub> at 200 and  $100^\circ\text{C}$ . The results (not reported here) showed behavior quite similar to that of curve (C) for the sample pretreated at  $200^\circ\text{C}$ , whereas with pretreatment at  $100^\circ\text{C}$ , the catalyst behaved like the reference reduced sample and thus likely was not oxidized. Accordingly, the temperature threshold for catalyst reoxidation

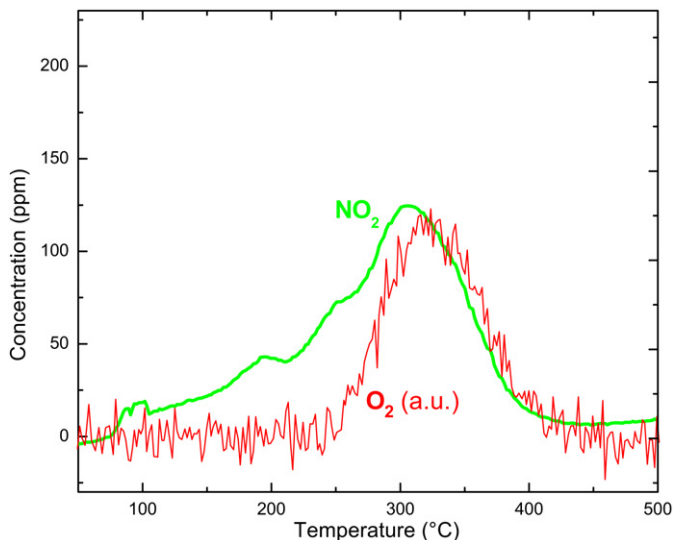


Fig. 4.  $\text{NO}_2$  and  $\text{O}_2$  concentration profiles during  $T$ -ramp at  $20^\circ\text{C}/\text{min}$  after catalyst pretreatment with  $\text{HNO}_3$  ( $\sim 100$  ppm) at  $150^\circ\text{C}$ . Feed flow rate =  $280\text{ cm}^3/\text{min}$  (STP).

by  $\text{HNO}_3$  lies between  $100$  and  $150^\circ\text{C}$  under our experimental conditions.

Another important feature becomes apparent on inspection of Fig. 3. For the catalyst samples pretreated with  $\text{NO}_2$  and  $\text{HNO}_3$  (curves (B) and (C), respectively), the behavior during the  $\text{NO} + \text{NH}_3$  temperature ramp was identical to that of the TPR run over the reference oxidized catalyst (curve D) up to about  $170^\circ\text{C}$ ; above this temperature, however, curves (B) and (C) exhibited a marked increment of  $\text{deNO}_x$  activity, followed by a sudden drop in  $\text{NO}$  conversion at around  $250^\circ\text{C}$ . Interestingly, such a temperature threshold corresponds to the onset of nitrate decomposition, as indicated by the main desorption peaks of  $\text{O}_2$  and  $\text{NO}_2$  detected during TPD runs after buildup of nitrates onto the catalyst by exposure to either  $\text{HNO}_3$  (see Fig. 4) or  $\text{NO}_2$  (with similar results). The formation/storage of nitrate species onto pure  $\text{TiO}_2$ ,  $\text{WO}_3/\text{TiO}_2$ , and  $\text{V}_2\text{O}_5\text{-WO}_3/\text{TiO}_2$  catalysts from  $\text{NO}_2$  has been reported by several authors [35–38]. Thus, Figs. 3 and 4 provide evidence in favor of a strong promoting action of adsorbed nitrates on the  $\text{NO} + \text{NH}_3$  SCR reactivity at low temperature. The surface nitrates would then be decomposed and depleted above  $\approx 250^\circ\text{C}$ , explaining the subsequent drop in  $\text{NO}$  conversion.

### 3.6. Mechanistic implications: catalyst reoxidation and role of nitrates

As for the catalyst reduction step in Section 4, herein we discuss the results of Figs. 3 and 4 in relation to their relevant mechanistic implications. So far, only Raman evidence has been reported in the literature to support that  $\text{NO}_2$  affects the reoxidation of V-based SCR catalysts more efficiently than gaseous oxygen [17]. In this respect, the data in Fig. 3 provide a direct confirmation that  $\text{NO}_2$  can reoxidize the reference reduced catalyst at a much lower temperature than  $\text{O}_2$  under SCR reactive conditions. They further prove that  $\text{HNO}_3$  is a much better oxidizing agent as well.

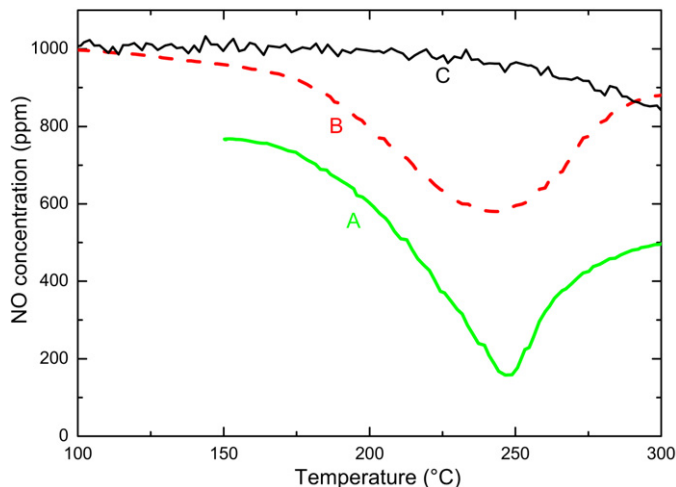


Fig. 5.  $\text{NO}$  concentration profiles during  $T$ -ramps at  $20^\circ\text{C}/\text{min}$ . Curve (A) feed =  $\text{NO} + \text{NH}_3 + \text{NO}_2$  ( $1000/1000/500$  ppm). Curve (B) feed =  $\text{NO} + \text{NH}_3$  ( $1000/1000$  ppm) over reduced catalyst pretreated with  $\text{NO}_2$  ( $500$  ppm) at  $150^\circ\text{C}$ . Curve (C) feed =  $\text{NO} + \text{NH}_3 + \text{O}_2$  ( $1000/1000/500$  ppm).

Because catalyst reoxidation is the rate-limiting step of the SCR reaction, as documented in Section 2, an important implication is that the overall SCR  $\text{deNO}_x$  kinetics will be strongly enhanced in the presence of  $\text{NO}_2$  and/or  $\text{HNO}_3$ . In fact, the promoting action of  $\text{NO}_2$  when added to the  $\text{NO} + \text{NH}_3$  reacting system, leading to the so-called fast SCR, is well known in the SCR literature.

Notably, the behavior observed after oxidizing the catalyst with either  $\text{NO}_2$  or  $\text{HNO}_3$  was similar. In fact, as presented and discussed in other works from our group [13,23,24], over V-based SCR systems at low temperatures  $\text{NO}_2$  readily undergoes the disproportionation reaction



so that the reactivities of  $\text{NO}_2$  and  $\text{HNO}_3$  can hardly be distinguished.

Fig. 3 further suggests that the buildup of nitrates onto the V-based catalyst (possibly onto sites associated with the W and Ti components) may play an important role in enhancing the  $\text{deNO}_x$  efficiency compared with the  $\text{NO} + \text{NH}_3 + \text{O}_2$  standard SCR below  $250^\circ\text{C}$ . In this respect we have previously reported evidence pointing to a significant participation of nitrates in the mechanism of the fast SCR reaction; specifically, data from dedicated transient reactivity experiments at  $170^\circ\text{C}$  showed that the rate of fast SCR (2) equals the rate of reduction of nitrate species (related to  $\text{NH}_4\text{NO}_3$ ) by  $\text{NO}$  [23,24].

Additional transient experiments illustrated in Fig. 5 provide more insight into the role of nitrates in the catalyst reoxidation step, and also into its relationship with the rate of fast SCR. In Fig. 5, curve (A) represents the evolution of  $\text{NO}$  conversion observed during a TPR run at  $150\text{--}300^\circ\text{C}$  with a feed including  $\text{NO}$  ( $1000$  ppm) +  $\text{NO}_2$  ( $500$  ppm) +  $\text{NH}_3$  ( $1000$  ppm). At  $150^\circ\text{C}$ , the  $\text{NO}$  conversion was  $>20\%$  due to the fast SCR reaction. At this low temperature, however,  $\text{NO}_2$  and  $\text{NH}_3$  also reacted to form  $\text{NH}_4\text{NO}_3$ , which partially built up onto the

catalyst [13,24], as pointed out by the following analysis of ammonia, NO<sub>2</sub>, and nitrogen traces (not shown in the figure):



With increasing temperature up to about 250 °C, NO conversion was significantly enhanced, eventually exceeding 80%. Notably, this is higher than the stoichiometric limit of 50% associated with the feed concentration of NO<sub>2</sub>, a clear indication that the reaction proceeded at the expense of nitrates initially stored on the catalyst. In fact, NO conversion again dropped suddenly when the temperature exceeded 250 °C (i.e., the temperature threshold corresponding to the onset of nitrate decomposition [see Fig. 4]), and eventually approached the steady-state stoichiometric 50% limit.

Curve (B) in Fig. 5 displays the evolution of NO conversion during a temperature ramp in which only NO and NH<sub>3</sub> (1000 ppm each) were fed over a reduced catalyst sample that had been previously pretreated with NO<sub>2</sub> (500 ppm). The similarity between curves (A) and (B) is quite evident. In particular, in the range 150–225 °C the temperature dependence of the fast SCR reaction in the presence of gaseous NO<sub>2</sub> (as inferred from curve (A)) is virtually the same of the NO + NH<sub>3</sub> reaction in the presence of adsorbed nitrates (curve (B)). This strongly suggests that, as in standard SCR, the rate-determining step in the fast SCR reaction is still associated with reoxidation of the V sites, which is, however, accomplished more effectively by adsorbed nitrates generated from NO<sub>2</sub> than by gaseous oxygen, as in the case of standard SCR.

For comparison purposes, Fig. 5 displays also curve (C) (same as curve (A) in Fig. 1) associated with NO conversion during a NO + NH<sub>3</sub> + O<sub>2</sub> temperature ramp. The drastically lower reactivity of NO in standard SCR, in the absence of either gaseous NO<sub>2</sub> (as in curve (A)) or adsorbed nitrates (as in curve (B)), is clearly apparent.

We also note that replacing O<sub>2</sub> with gaseous NO<sub>2</sub> in the role of V-oxidizing agent, as proposed by Koebel et al. [17] to account for the higher fast SCR rates, cannot explain the transient data of the temperature ramps in Figs. 3 and 5. Instead, V reoxidation must be effected by adspecies stored on the catalyst, either nitrates or possibly molecularly adsorbed NO<sub>2</sub>. Such adsorbed species act as reservoirs of oxidizing agents, thus permitting the significant increment of NO conversion observed as the temperature is raised.

### 3.7. Role of vanadium redox properties in the fast SCR reaction

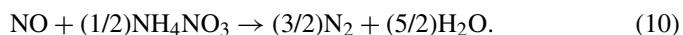
Data reported in the previous sections showed that buildup of nitrates onto the V-based catalyst plays a crucial role in enhancing SCR deNO<sub>x</sub> efficiency. It was suggested that this results from the fact that nitrates reoxidize the vanadium sites more efficiently than gaseous oxygen. However, nitrates also are formed onto sites related to W and Ti [35], the most abundant components of the SCR catalyst. Accordingly, to assess the role of vanadium (in particular, its redox properties) in the mechanism of the fast SCR reaction, more dedicated transient runs were carried out on a comparative basis over the V-based

catalyst discussed earlier, as well as over a commercial V-free WO<sub>3</sub>/TiO<sub>2</sub> catalyst. The experiments were designed to analyze separately the two consecutive reaction steps—nitrate buildup and their reduction by NO—that previous works identified as the two major stages in the mechanism of the overall fast SCR reaction at low temperatures [23,24].

Fig. 6A shows the experiment performed over the V-based catalyst at 170 °C [23]. In the first stage, NH<sub>3</sub> and NO<sub>2</sub> alone were fed to the reactor, thereby forming and depositing ammonium nitrate onto the catalyst as confirmed by the consumption of both reactants and the production of nitrogen, in agreement with reaction (9). Formation of ammonium nitrate, as estimated from the lack in nitrogen balance, was also in line with (9). DTA-TG measurements confirmed that the endothermic decomposition of ammonium nitrate did not start until 173–174 °C, slightly above the temperature of the present experiment. Thus, the formed NH<sub>4</sub>NO<sub>3</sub> remained on the catalyst sample.

The second part of the run involved removing NO<sub>2</sub> from the feed stream. Thus NH<sub>3</sub> readily recovered its feed concentration level, and the reaction was no longer observed, even though residual ammonium nitrate was still present on the catalyst. Afterwards, NO was admitted to the reactor while ammonia was still continuously fed ( $t = 8500$  s); NO and NH<sub>3</sub> immediately reacted in equimolar amounts, with production of N<sub>2</sub>. But the reaction also involved consumption of NH<sub>4</sub>NO<sub>3</sub> and in fact proceeded only until depletion of the ammonium nitrate deposited onto the catalyst.

Data from this and other similar experiments [24] have been interpreted assuming that the conversion of ammonium nitrate occurred via the reaction between NO and nitric acid (in equilibrium with ammonium nitrate), which was thus reduced to nitrous acid with formation of NO<sub>2</sub>. Then in the presence of adsorbed NH<sub>3</sub>, nitrous acid would produce N<sub>2</sub> via decomposition of NH<sub>4</sub>NO<sub>2</sub>, whereas NO<sub>2</sub> would react readily with ammonia to form more NH<sub>4</sub>NO<sub>3</sub> and N<sub>2</sub> [24]. Such a scheme is in fact in agreement with the observed overall stoichiometry,



To analyze the role of vanadium in this global reactivity, an identical experiment was run over the V-free WO<sub>3</sub>/TiO<sub>2</sub> catalyst (Fig. 6B). The first part of this experiment shows that feeding NH<sub>3</sub> and NO<sub>2</sub> to the reactor resulted in nitrogen production, similar to what was seen over the V-based catalysts and in agreement with reaction (9), indicating that formation and deposition of ammonium nitrate occurred over the WO<sub>3</sub>/TiO<sub>2</sub> catalyst, just as for the V-based catalyst. Accordingly, vanadium seems unnecessary for the formation of ammonium nitrate onto the catalyst surface.

A very different picture appears in the second and final part of the experiment, when NO was admitted to the reactor (roughly at  $t = 8250$  s). In contrast to the V-based catalyst (Fig. 6A), on feeding NO to the WO<sub>3</sub>/TiO<sub>2</sub> catalyst, where nitrates had been stored previously, here we found no conversion of either nitric oxide or ammonia, or any nitrogen production. This indicates that the V-free sample did not allow reduction of nitrate species by NO, at least under the experimental condi-

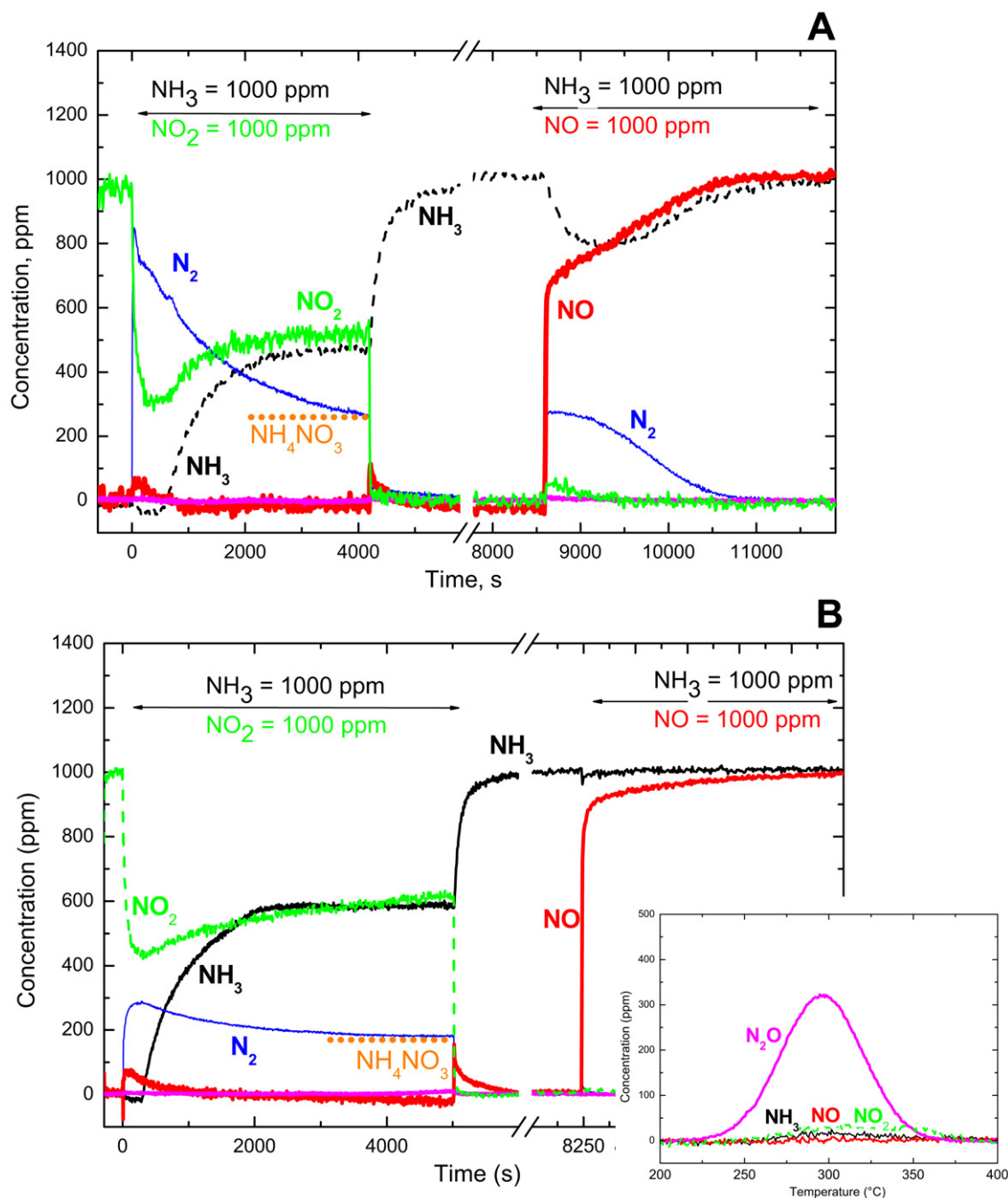


Fig. 6. Transient experiments at  $T = 170^\circ\text{C}$ : formation of  $\text{NH}_4\text{NO}_3$  (feed: 1000 ppm  $\text{NH}_3$ , 1000 ppm  $\text{NO}_2$ , 1%  $\text{H}_2\text{O}$ ); reduction of  $\text{NH}_4\text{NO}_3$  by NO (feed: 1000 ppm  $\text{NH}_3$ , 1000 ppm NO, 1%  $\text{H}_2\text{O}$  in He). (A)  $\text{V}_2\text{O}_5\text{-WO}_3/\text{TiO}_2$  catalyst; (B)  $\text{WO}_3/\text{TiO}_2$  catalyst. Inset: TPD run performed at the end of experiment (B).

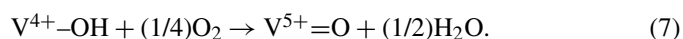
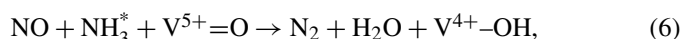
tions used here. Notably, the presence of unreacted  $\text{NH}_4\text{NO}_3$  on the V-free catalyst sample was confirmed by an additional TPD experiment performed at the end of this run (see Fig. 6B, inset). Heating the  $\text{WO}_3/\text{TiO}_2$  catalyst in inert atmosphere provoked the decomposition of the residual ammonium nitrate, leading primarily to the evolution of  $\text{N}_2\text{O}$  [11,22,24].

### 3.8. A unifying redox scheme for standard SCR and fast SCR

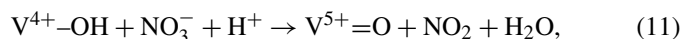
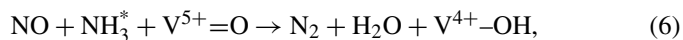
Herein we propose a set of reactions that formally summarizes the catalytic chemistry underlying the experiments dis-

cussed thus far and, by identifying the related role of the vanadium redox properties, provides a unifying approach to the mechanisms of the standard SCR and fast SCR reactions.

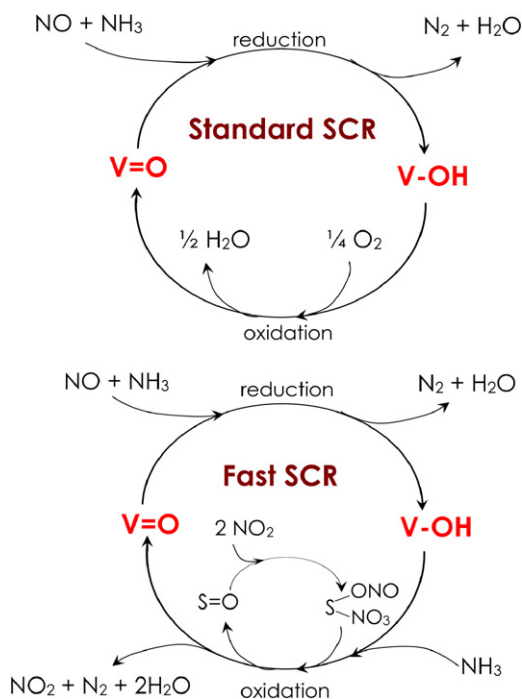
#### Standard SCR:



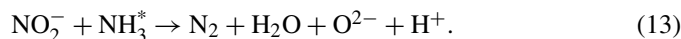
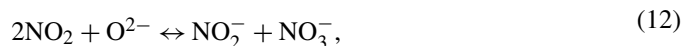
#### Fast SCR:







Scheme 1. Redox catalytic cycles of the standard and fast SCR reactions over  $V_2O_5$ - $WO_3$ / $TiO_2$  catalysts.  $V=O$  and  $V-OH$  are oxidized and reduced vanadium sites, respectively.  $S=O$  is a non-reducible oxidic site.



The steps associated with the  $NO + NH_3 + O_2$  standard SCR, reactions (6) and (7), were discussed in Section 4. Reaction (6) accounts for reduction of the  $V^{5+}$ -sites; reaction (7) is the rate-limiting reoxidation step involving gaseous oxygen.

In the case of the  $NO + NH_3 + NO_2$  fast SCR, the reduction of the V sites still occurs according to the same global reaction (6), but the rate-determining step in the redox process (i.e., the reoxidation of V sites) is radically changed, in this case being carried out by surface nitrates according to reaction (11), which replaces the much slower reaction (7). The introduction of nitrates brings about additional complexity to the SCR chemistry, however, so reaction (12) represents formation of nitrite and nitrate ad-species via disproportion of  $NO_2$ , whereas reaction (13) accounts for the decomposition of nitrites to  $N_2$  via reaction with  $NH_3$ . In agreement with the experimental observations shown in Fig. 6, no redox catalyst function is involved in steps (12) and (13), which are assumed to occur over nonreducible oxidic sites, represented here schematically as  $O^{2-}$ , possibly associated with the W- or Ti-catalyst components. A similar sequence has been invoked in the literature to explain the formation of ammonium nitrate from  $NO_2 + NH_3$  observed over  $TiO_2$  [35] and over zeolites [25], as well as the formation of nitrates from  $NO_2$  over  $Al_2O_3$  [39]. The redox cycles of the vanadium sites for the standard SCR and fast SCR reactions are schematically depicted in Scheme 1.

In summary, the proposed redox mechanism:

- (i) Explains the higher rate of the fast SCR as due to the faster reoxidation of V sites by nitrates (see Fig. 3).
- (ii) Agrees with the behavior observed during transient runs, when the fast SCR occurred also in the absence of gaseous  $NO_2$  due to the involvement of surface nitrates (see Fig. 5).
- (iii) Is consistent with the reducing action of NO on adsorbed nitrates and ammonium nitrate, observed and reported herein (Fig. 6A) and in previous publications [13,23,24], and explains why this reaction does not proceed effectively on a V-free catalyst (Fig. 6B).
- (iv) Can account not only for the  $deNO_x$  reactions, but also for the formation of observed byproducts, such as ammonium nitrate and  $N_2O$ , both originating from reactions of surface nitrates with ammonia at low and high temperatures, respectively [12,13,23,24].

#### 4. Conclusion

$NO + NH_3$  TPR runs in the absence of oxygen were used to examine mechanistic features of the SCR reaction over an industrial V-based catalyst for diesel exhaust aftertreatment under representative low-temperature conditions. Through such methods, we have confirmed that reoxidation of the vanadium sites by gaseous oxygen is the rate-limiting step in the redox catalytic mechanism of the standard SCR ( $NO + NH_3 + O_2$ ) reaction.

However, the main contribution of the present work concerns the mechanism of the less well-investigated fast SCR ( $NO + NH_3 + NO_2$ ) reaction. TPR data offer direct experimental evidence that reoxidation of V sites is significantly accelerated in the presence of  $NO_2$  and/or  $HNO_3$ ; this explains why fast SCR is so much faster than standard SCR at low temperatures. Our data further suggest that this is not a direct effect, as was previously proposed in the literature, but rather results from the crucial participation of nitrates adspecies, formed from  $NO_2$ , in reoxidizing the reduced V sites and thus in promoting the rate of the SCR reaction over V-based catalysts. This aspect is critical to rationalize the transient behavior of the fast SCR reacting system and for SCR dynamic kinetic modeling.

The present results open the way to a new interpretation of the complete  $NO/NO_2-NH_3$  low-temperature catalytic chemistry involved in both the standard and fast SCR reactions over V-based catalysts. It relies on a unifying redox approach in which the rate-controlling reoxidation of the vanadium catalyst sites involves gaseous oxygen in the  $NH_3$  SCR of NO only, but is carried out more effectively by surface nitrates when  $NO_2$  is added to the reacting system. Nitrates are formed via disproportion of  $NO_2$  in a secondary catalytic cycle that does not require a redox function.

To the best of our knowledge, this redox scheme is consistent with most experimental observations concerning  $NH_3$ -SCR chemistry over V-based catalysts available in the literature. It may prove useful as well to interpret mechanistic data for  $NH_3$ -SCR over zeolite-based catalysts. A transient Mars–Van Krevelen kinetic model in close agreement with the SCR chemistry discussed herein is currently under development.

## References

- [1] ACEA final report on Selective Catalytic Reduction, June 2003, [http://europa.eu.int/comm/enterprise/automotive/mveg\\_meetings/meeting94/scr\\_paper\\_final.pdf](http://europa.eu.int/comm/enterprise/automotive/mveg_meetings/meeting94/scr_paper_final.pdf).
- [2] M. Koebel, M. Elsener, M. Kleemann, *Catal. Today* 59 (2000) 335.
- [3] R.M. Heck, R.J. Farrauto, S.T. Gulati, in: *Catalytic Air Pollution Control*, second ed., Wiley, New York, 2002.
- [4] <http://www.cleers.org>.
- [5] [http://www4.mercedes-benz.com/specials/scr/en/scr\\_start\\_e.swf](http://www4.mercedes-benz.com/specials/scr/en/scr_start_e.swf).
- [6] <http://www.sae.org/automag/features/futurelook/01-2005/1-113-1-84.pdf>.
- [7] <http://www.volvo.com/group/scr/en-gb/>.
- [8] <http://www.renault-trucks.it/>.
- [9] P. Forzatti, L. Lietti, E. Tronconi, in: I.T. Horvath (Ed.), *Nitrogen Oxides Removal—Industrial*. Encyclopedia of Catalysis, first ed., Wiley, New York, 2002, and references therein.
- [10] A. Kato, S. Matsuda, T. Kamo, F. Nakajima, H. Kuroda, T. Narita, *J. Phys. Chem.* 85 (1981) 4099.
- [11] M. Koebel, G. Madia, M. Elsener, *Catal. Today* 73 (2002) 239.
- [12] G. Madia, M. Koebel, M. Elsener, A. Wokaun, *Ind. Eng. Chem. Res.* 41 (2002) 351.
- [13] C. Ciardelli, I. Nova, E. Tronconi, B. Bandl-Konrad, D. Chatterjee, M. Weibel, B. Kruttsch, *Appl. Catal. B Environ.* (2006), in press, doi:10.1016/j.apcatb.2005.10.041.
- [14] G. Busca, L. Lietti, G. Ramis, F. Berti, *Appl. Catal. B* 18 (1998) 1, and references therein.
- [15] L. Lietti, P. Forzatti, *J. Catal.* 147 (1994) 241.
- [16] L. Lietti, P. Forzatti, F. Bregani, *Ind. Eng. Chem. Res.* 35 (1996) 3884.
- [17] M. Koebel, G. Madia, F. Raimondi, A. Wokaun, *J. Catal.* 209 (2002) 159.
- [18] I. Nova, C. Ciardelli, E. Tronconi, D. Chatterjee, B. Bandl-Konrad, *AIChE J.* 52 (2006) 3222.
- [19] N.-Y. Topsøe, J.A. Dumesic, H. Topsøe, *J. Catal.* 151 (1995) 241.
- [20] V.I. Marshneva, E.M. Slavinskaya, O.V. Kalinkina, G.V. Odegova, E.M. Moroz, G.V. Lavrova, A.N. Salanov, *J. Catal.* 155 (1995) 171.
- [21] M. Koebel, M. Elsener, G. Madia, *Ind. Eng. Chem. Res.* 40 (2001) 52.
- [22] G. Madia, M. Koebel, M. Elsener, A. Wokaun, *Ind. Eng. Chem. Res.* 41 (2002) 4008.
- [23] C. Ciardelli, I. Nova, E. Tronconi, D. Chatterjee, B. Bandl-Konrad, *Chem. Commun.* 23 (2004) 2718.
- [24] I. Nova, C. Ciardelli, E. Tronconi, D. Chatterjee, B. Bandl-Konrad, *Catal. Today* 114 (2006) 3.
- [25] G.T. Went, L.-J. Leu, S.J. Lombardo, A.T. Bell, *J. Phys. Chem.* 96 (1992) 2235.
- [26] Y. Yeom, J. Henao, M. Li, W.M.H. Sachtler, E. Weitz, *J. Catal.* 231 (2005) 181.
- [27] I. Giakoumelou, C. Fountzoula, C. Kordulis, S. Boghosian, *J. Catal.* 239 (2006) 1.
- [28] C. Ciardelli, I. Nova, E. Tronconi, B. Konrad, D. Chatterjee, K. Ecke, M. Weibel, *Chem. Eng. Sci.* 59 (2004) 5301.
- [29] D. Chatterjee, T. Burkhardt, B. Bandl-Konrad, T. Braun, E. Tronconi, I. Nova, C. Ciardelli, SAE technical paper 2005-01-965 (2005).
- [30] E. Tronconi, I. Nova, C. Ciardelli, D. Chatterjee, T. Burkhardt, B. Bandl-Konrad, *Catal. Today* 105 (2005) 529.
- [31] D. Chatterjee, T. Burkhardt, M. Weibel, E. Tronconi, I. Nova, C. Ciardelli, SAE technical paper 2006-01-0468 (2006).
- [32] R.J. Willey, J.W. Elridge, J.R. Kittrell, *Ind. Eng. Chem. Prod. Res. Dev.* 24 (1985) 226.
- [33] F. Kapteijn, L. Singoredjo, N.J.J. Dekker, J.A. Moulijn, *Ind. Eng. Chem. Res.* 32 (1993) 445.
- [34] I. Nova, L. Lietti, E. Tronconi, P. Forzatti, *Catal. Today* 60 (2000) 73.
- [35] J. Despres, M. Koebel, O. Krocher, M. Elsener, A. Wokaun, *Appl. Catal. B Environ.* 43 (2003) 389.
- [36] S. Djerad, M. Crocoll, S. Kureti, L. Tifouti, W. Weisweiler, *Catal. Today* 113 (2006) 208.
- [37] G. Piazzesi, O. Krocher, M. Elsener, A. Wokaun, *Appl. Catal. B Environ.* 65 (2006) 55.
- [38] G. Piazzesi, O. Krocher, M. Elsener, A. Wokaun, *Appl. Catal. B Environ.* 65 (2006) 169.
- [39] N. Apostolescu, T. Schroder, S. Kureti, *Appl. Catal. B Environ.* 51 (2004) 43–50.